M&C 2017 - International Conference on Mathematics & Computational Methods Applied to Nuclear Science & Engineering, Jeju, Korea, April 16-20, 2017, on USB (2017)

Preliminary Simulation Results of BEAVRS Three-dimensional Cycle 1 Wholecore Depletion by UNIST Monte Carlo Code MCS

[a]Hyunsuk Lee, [a]Wonkyeong Kim, [a]Peng Zhang, [a]Azamat Khassenov, [a]Jinsu Park, [a]Jiankai Yu, [a]Sooyoung Choi, [b]Hwan Soo Lee and [a]Deokjung Lee[*]

[a] *Department of Nuclear Engineering, UNIST, UNIST-gil 50, Ulsan 44919, Republic of Korea*
[b]*Core and Fuel Analysis Group, KHNP-CRI, 70, Yuseong-daero, Yuseong-gu, Daejeon 34101, Republic of Korea*
[*] *Corresponding author: deokjung@unist.ac.kr*

Abstract - *This paper presents the preliminary solutions of BEAVRS cycle 1 depletion by Monte Carlo (MC) code MCS developed at Ulsan National Institute of Science and Technology (UNIST). The simulation was performed with five feedback modules required for power reactor simulation: Thermal-Hydraulics (TH), depletion, equilibrium xenon, Critical Boron Concentration (CBC) and On-The-Fly (OTF) cross-section reconstruction. The CBC and radial detector signal map were compared with the reference data in BEAVRS 2.0 document. The power, flux, fuel temperature and coolant temperature distributions are presented. The CBC and detector signals are compared with measured data. It is shown that MCS can estimate the CBC with a maximum deviation of 100 ppm, and that MCS can calculate detector signals accurately with 2-5% RMS error.*

I. INTRODUCTION

The Monte Carlo (MC) method has the advantages of accurate geometry tracking and exact treatment of continuous energy cross section. The main difficulty for the wide and extensive application of the MC simulation is that the MC requires huge amount of memory and computing time to simulate the commercial reactor design. As computing power increases and the demands of high-fidelity simulation increases, the MC simulation has been more and more popular and feasible.

Around the world, various groups have been trying to achieve the high fidelity whole core direct calculation, either by deterministic or by the Monte Carlo codes. The BEAVRS benchmark is proposed to better promote the development. For the direct 3D whole core calculation, the Monte Carlo codes show some advantages over the deterministic codes, and so more and more attention has been paid on the MC code development. UNIST has also been developing the MC code named MCS to satisfy this demand of high-fidelity simulation [1-2]. In this paper, the preliminary solution of BEAVRS cycle 1 is presented to demonstrate the capability of MCS to be used for the commercial reactor analysis, which requires various feedbacks, including Thermal-Hydraulics (TH), depletion, equilibrium xenon, Critical Boron Concentration (CBC), and On-The-Fly (OTF) cross-section reconstruction [3-9].

II. FEEDBACKS

MCS updates the TH condition, xenon number density, and boron concentration every cycle based on the parameters tallied during each cycle. After finishing each step criticality simulation, the number density will be updated. The flow chart of MCS is shown Fig. 1.

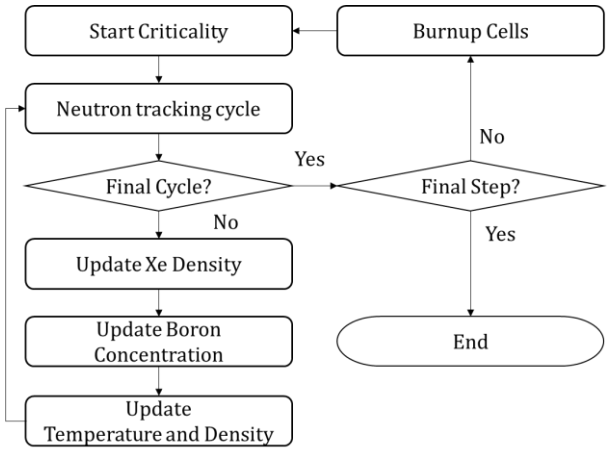

Fig. 1. Flow chart of MCS.

II.1. Thermal-Hydraulics (TH) Feedback

The one-dimensional TH module (TH1D) has been implemented [3]. The TH1D module receives the power distribution for each pin from MC module and returns the temperature and density distribution to MC module. TH1D calculates TH solution for each pin one by one and cross-flow effect cannot be considered.

The TH-coupling is performed every cycle and therefore sometimes the power used for TH1D may be unphysical because of large statistical fluctuations. To prevent this issue, MCS has internal checking routines to prevent unphysical results. The statistical issue will be discussed later.

II.2. Temperature Dependent Cross Sections

The OpenW module developed at MIT CRPG has been implemented [4-5]. The OpenW module is an OTF cross section generation module based on the multipole representation of resonance parameters. The OpenW module can be used to get the Doppler broadened cross-section in resonance range. Currently, this can be used only for the 72 nuclides. MIT is working to extend to all nuclides, and UNIST is also trying to develop own OTF library. The nuclides which are not in the OpenW library can be treated with SIGMA1 kernel. SIGMA1 kernel generates the ACE format file before the transport calculation [6-7].

II.3. Equilibrium Xenon

It is known that the Xenon number density and flux can be fluctuating during depletion of high dominance problem [8-9]. This oscillation can be suppressed by updating number density of Xe-135 based on the cycle tallied quantities. MC tallies flux and reaction rates for depletion, and it can be used to update number density as follow

$$N_{Xe} = \frac{\gamma_{Xe} \Sigma_f \phi}{\lambda_{Xe} + \sigma_{Xe,a}\phi} , \qquad (1)$$

where γ_{Xe} is the cumulative fission yield of Xe-135 which include the yield of I-135, Σ_f is the macroscopic fission cross section, ϕ is the flux, λ_{Xe} is the decay constant of Xe-135, and $\sigma_{Xe,a}$ is the microscopic absorption cross section of Xe-135.

II.4. Depletion

The code has a built-in depletion module which can efficiently treat the massive burnup calculation. The detailed burnup chain consists of 1,374 nuclides including actinides, activation products, and fission products. The large system of linear equations with those nuclides can be solved with high accuracy and efficiency by Chebyshev Rational Approximation Method (CRAM). The depletion module has a capability of parallel depletion calculation for large-scale problems. Full- and semi- predictor-corrector methods are available for the burnup calculation.

III. RESULTS

This section is composed of 6 parts: benchmark description, stability study of feedbacks, memory requirement, BOC result, cycle 1 depletion result, and the detector signal comparison.

III.1. Benchmark Description

BEAVRS (Benchmark for Evaluation and Validation of Reactor Simulation) was published by MIT [3,10]. It is PWR benchmark contains very detailed information which is composed of 50,952 fuel pins. Fig. 2 shows the radial and axial geometry images of BEAVRS core generated by MCS.

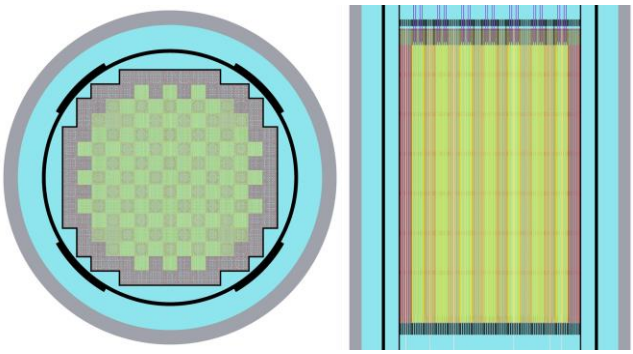

Fig. 2. BEAVRS core generated by MCS.

III.2. Stability Issue of TH feedbacks

MCS updates TH conditions every cycle based on the parameters tallied during one cycle. This strategy can cause the stability issue because of large statistical error. If the statistical error of power is too high, the TH solver may diverge or it may give unphysical output such as negative density or very high temperature. MCS checks the output of TH solver, and it is considered as unphysical solution if the highest fuel temperature is higher than 2000K or the water density is negative. There was no unphysical TH output observed for all simulations performed for this paper. In addition, the fluctuation of fuel temperature is smaller than the fission source distribution.

The TH output calculated using one cycle tally is used for the transport calculation. And the final temperature result will be the average of active cycles and standard deviation. The number of inactive cycle was determined with Shannon entropy calculated using fuel temperature information.

III.3. Memory Requirement

The issue of Monte Carlo simulation is always computing time in general. Depending on the complexity of the problem and the target statistical error, MC simulation may take forever to be done. In addition to this issue, the memory requirement is also an important issue for depletion/TH simulation.

The number of data required per one cell containing 251 nuclides is as follow

- Reaction rates (9 reactions) for scoring:
  $251 \times 9 = 2{,}259$

- Reaction rates (9 reactions) for statistical process: $251 \times 9 \times 2 = 4{,}518$
- Number density used in CRAM: 1,374
- Number density used in previous step (for predictor-corrector): 1,374

The reaction rates for scoring must be allocated in all processes, and the others can be allocated in one process. The size of ACE format cross section data for all nuclides is about 0.8GB, and this is also must be allocated in all processes. The memory requirement per one process will be determined number of burnup reasons, number of processes, and number of temperature points. And it can be calculated by Eq. (2).

$$M = N_{mesh} \times M_{all} + \frac{N_{mesh} \times M_{one}}{N_{processes}}, \qquad (2)$$

where N_{mesh} is number of depletion cell, M_{all} (=24,840 bytes) is the size of memory must be allocated to all processes, M_{one} (59,130 bytes) is the size of memory can be allocated in one process.

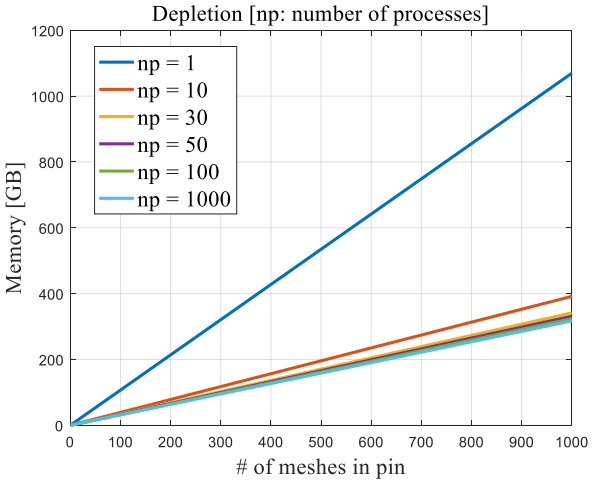

Fig. 3. Memory requirement per process.

The memory requirement per one process to solve quarter core geometry is shown in Fig. 3. The memory per process decreases as the number of processes increases.

III.4. BOC Results

The Beginning of Cycle (BOC) simulation was performed with a full core geometry. And the fuel pin was divided into 3 radial rings and 20 axial meshes.

The simulation was performed on a Linux cluster with 65 processes (Intel Xeon E5-2620 @ 3.00 GHz). Total 1.32 billion histories were used with 4 inactive cycles, 40 active cycles, 300 sub-cycles, and 100,000 histories per sub-cycle. TH feedback and xenon update subroutine were performed every cycle. Table I shows the multiplication factor, CBC, and the simulation time. It should be noted that MCS saved the ACE data every 50K, and use the closest data without broadening for the nuclide which is not in the OpenW data list.

Table I. Summary of BOC Simulation

Core power	3,411 MW
Inlet coolant temperature	560 °F
Pressure	2,250 psia
Core flow rate	61.5×106 kg/hr
Control rod position	ARO
k_{eff}	1.00001 ± 0.00004
CBC	660 ± 0.281 ppm
Simulation time	6.5 hours
# of processes	65

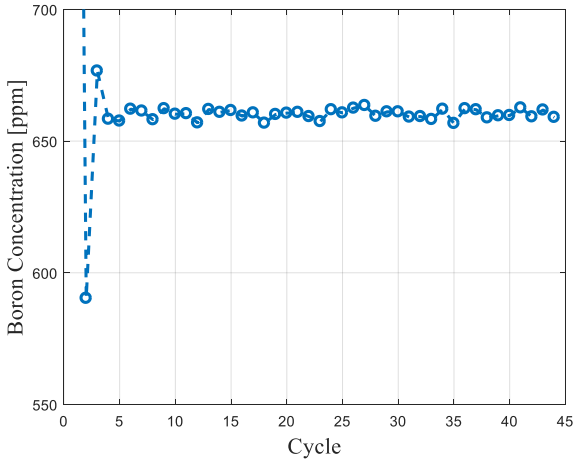

Fig. 4. Boron concentration.

The convergence of CBC, fission source and temperature distribution was checked as in Figs. 4-5. Fig. 4 shows the CBC estimated every cycle. The CBC converges after 3 cycles, and the fluctuation is small. Fig. 5 shows two Shannon entropies calculated with the fuel temperature and fission source. Both converged after 1 cycle since there are 300 sub-cycles, and the fluctuation of fuel temperature was smaller than that of fission source. It looks the TH feedback strategy is fine since there is no fuel pin diverged and small fluctuation of Shannon entropy.

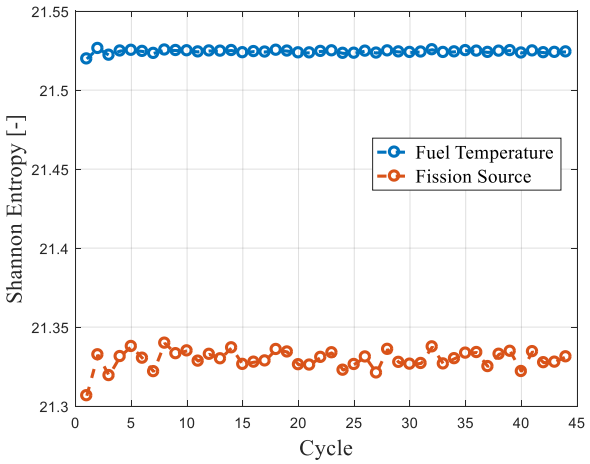

Fig. 5. Fuel temperature and fission source Shannon entropy.

Figs. 6-10 show the distribution of five different quantities: flux, fission reaction rate, fuel temperature, moderator density, moderator temperature. The quantities look reasonable.

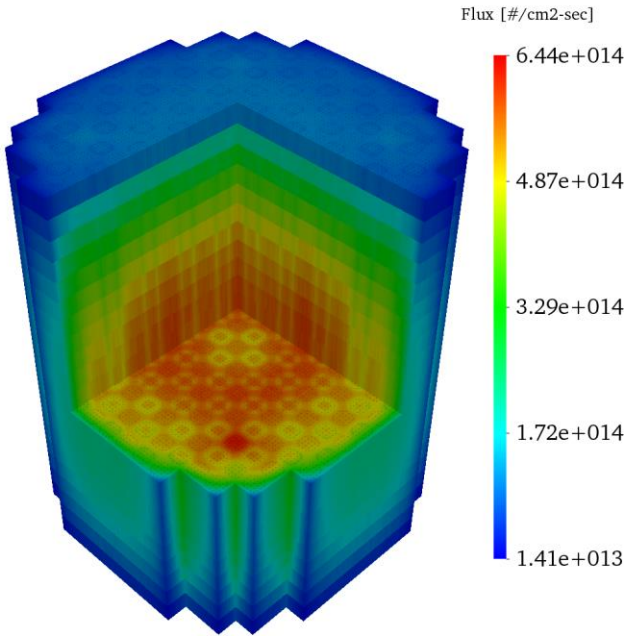

Fig. 6. Flux distribution.

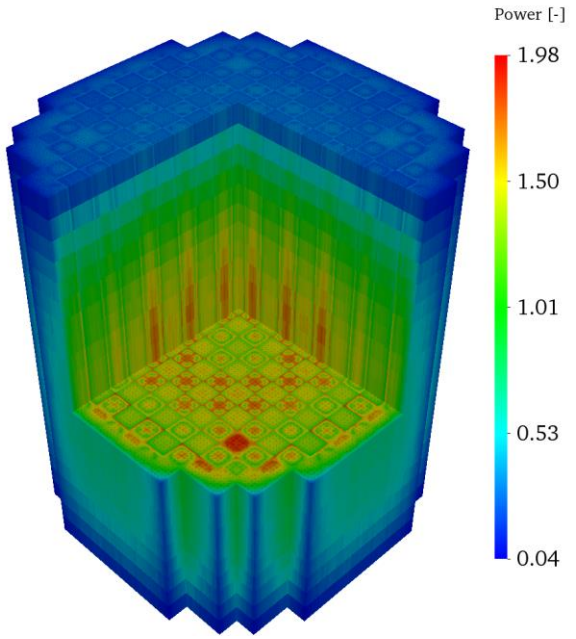

Fig. 7. Normalized power distribution.

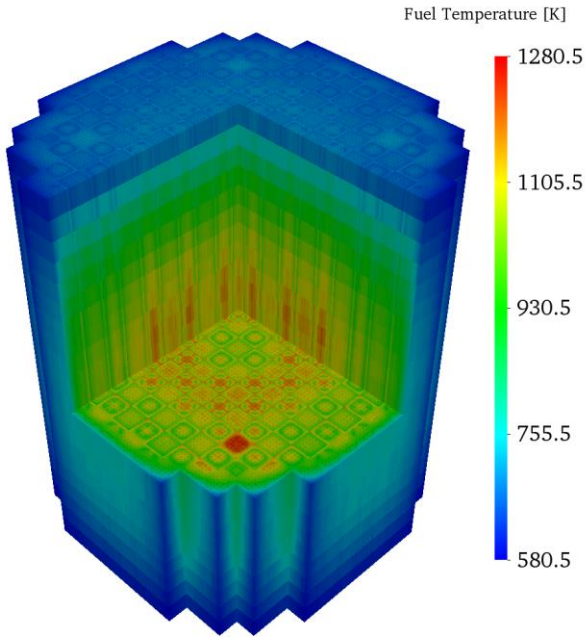

Fig. 8. Fuel temperature distribution.

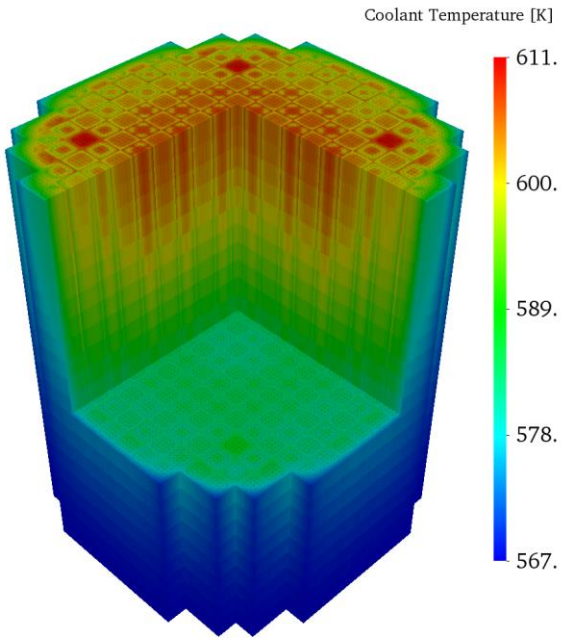

Fig. 9. Coolant temperature distribution.

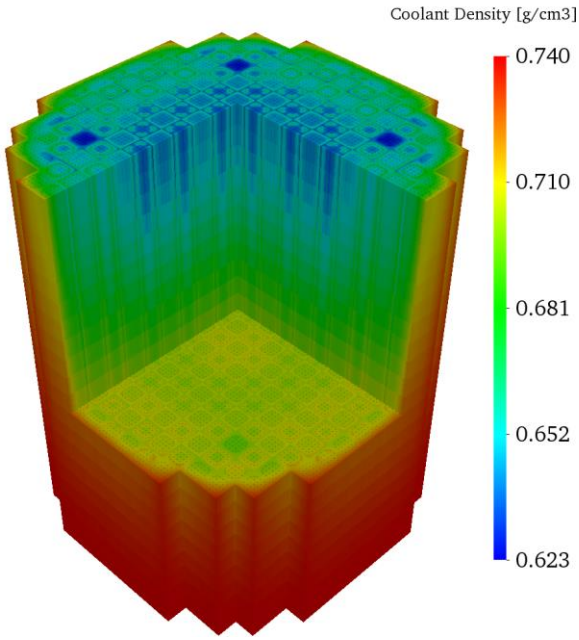

Fig. 10. Coolant density distribution.

III.5. Cycle 1 Depletion Results

The Cycle 1 simulation was performed with a quarter core geometry, and the fuel pin was divided into 1 radial ring and 10 axial meshes. All cases were simulated with 4 inactive cycles, 40 active cycles, 300 sub-cycle, and 10,000 histories per sub-cycle.

The simulation was performed on a Linux cluster with 65 processes (Intel Xeon E5-2620 @ 3.00 GHz). There are two quantities that can be used for the validation in the BEAVRS benchmark specification document: CBC and detector signals. It should be noted that MCS will use 600K ACE format data without considering broadening effect for the nuclides which is not in the OpenW library.

Three CBC tables are given in the benchmark document: Table 23, Table 25, and the pdf documents contains detector signals. Among three CBC tables, Table 25 and detector signals provide more details information that can be used for the simulation: inlet temperature, rod position, and power.

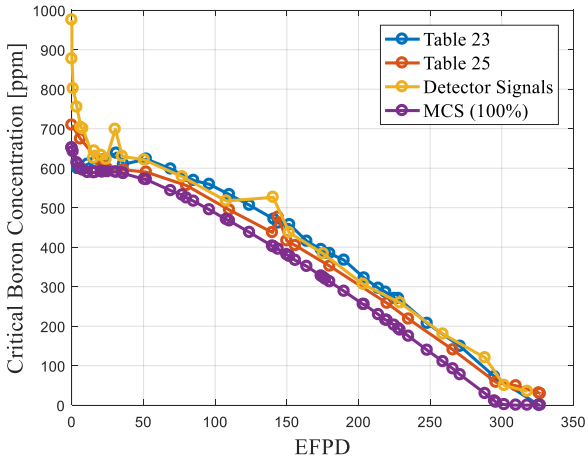

Fig. 11. Three CBC values in the BEAVRS document and MCS results.

The Cycle 1 simulation was performed with 100% power, constant inlet-temperature, and All Rod Out (ARO) condition to calculate the material composition that can be used to restart MCS. The number of depletion steps is 65 that can cover all the points that CBC data is given. For the depletion, semi-predictor corrector algorithm was used. Therefore 66 transport simulations were performed, and it took 6.5 days. The memory requirement per one process at EOC was about 3.5 GB. Fig. 11 shows the three CBC values in the benchmark document and the CBC result of MCS. It should be noted that the standard deviation of MCS CBC values are less than 1 ppm.

Simulations were performed again to produce the CBC and detector signals with conditions given in the benchmark document using the restart capability.

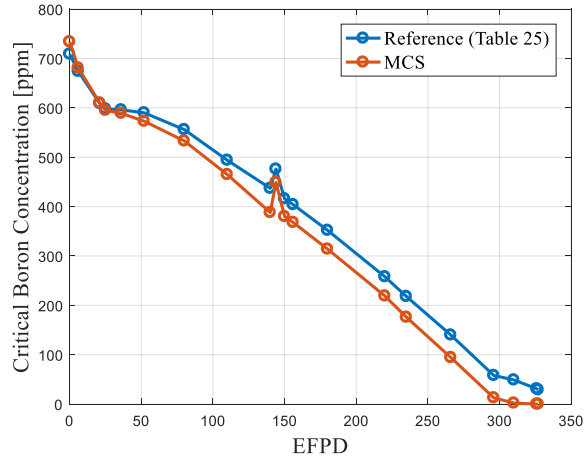

Fig. 12. Comparison of CBC in Table 25.

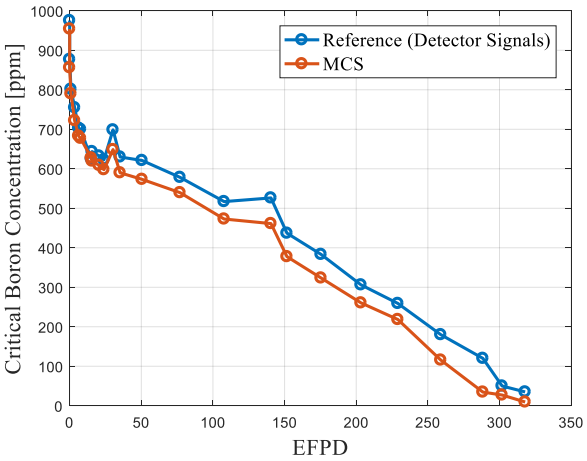

Fig. 13. Comparison of CBC in the detector signal document.

Figs. 12-13 show the result of restart with given condition. The MCS CBC result follows the trend of the reference graph very well, but MCS always underestimates the CBC with maximum 100 ppm difference. This result may be from the simplification of MCS simulation, and it may be from the assumptions and simplifications of the simulation which will be discussed in the section IV.

III.5. Detector Signal Comparison

BEAVRS benchmark provides the axially integrated detector signal map. In this paper, the tilt corrected radial detector map was compared with the result of MCS. The detector signal map from MCS was calculated by scoring fission reaction rate in the instrument tube filled with fission gas which is used only for the tallies not tracking. Table II shows the CBC for the 24 steps, and maximum and RMS value of detector signal difference. The standard deviation of detector signal is about 0.8-1.2%. Except for steps 2 and 6, the detector signal result matches well. Since it does not follow the detail power history because of the simulation time, the equilibrium xenon assumption was used. This significant discrepancy may come from this assumption, and it will be studied in the future. Figs. 14-23 show the power, flux, fuel temperature, coolant density, and detector signal comparison at BOC, MOC, EOC, step 2, and step 6. The results at BOC, MOC, and EOC show good agreements. Steps 2 and 6 show significant differences of detector signals due to the xenon number density issue.

Table II. Summary of Detector Signal Comparison.

Step	EFPD	CBC [ppm]			Detector Signal Rel. Diff.	
		Reference	MCS	SD	Max [%]	RMS [%]
1	0.00	975.25	953.98	0.001	-4.47	2.41
2	0.00	876.79	855.70	0.001	177.89	52.27
3	0.90	801.36	790.00	0.001	4.38	1.74
4	3.49	754.69	722.19	0.001	3.46	1.46
5	6.27	703.12	682.88	0.001	-4.79	2.36
6	7.63	700.00	677.19	0.001	80.88	16.65
7	15.07	625.15	627.58	0.001	-3.59	1.47
8	15.64	643.54	619.55	0.001	-3.44	1.70
9	20.53	632.38	608.81	0.001	2.80	1.32
10	23.91	622.62	597.69	0.001	6.50	2.43
11	30.27	698.50	648.57	0.001	-7.33	3.12
12	35.21	629.86	589.87	0.001	4.35	1.67
13	50.54	621.00	573.22	0.001	-3.26	1.58
14	77.05	578.23	539.50	0.001	-4.01	1.63
15	107.81	516.92	472.77	0.002	2.94	1.29
16	140.50	526.18	461.25	0.002	-5.96	2.03
17	151.67	436.92	377.51	0.002	-3.41	1.47
18	175.45	383.21	323.52	0.003	-5.67	2.31
19	203.33	306.09	260.45	0.003	-3.81	1.84
20	229.08	259.00	218.31	0.005	7.27	2.46
21	259.02	180.00	115.70	0.011	-4.94	1.97
22	288.40	120.00	34.60	0.036	-5.02	1.71
23	301.81	50.00	27.14	0.038	-6.16	2.38
24	317.90	35.00	9.53	0.129	-6.72	2.45

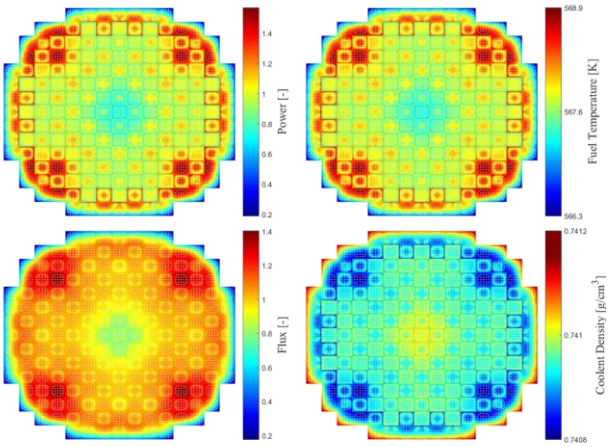

Fig. 14. Axially integrated quantities at the BOC (step 1): power, flux, fuel temperature, and coolant density.

-	0.78	1.07	0.94	1.15	0.94	1.27	0.78
-	0.79	1.09	0.92	1.16	0.92	1.25	0.76
-	1.73	1.73	-2.71	0.66	-1.71	-1.04	-2.71
0.78	1.01	0.90	1.15	0.98	1.17	0.84	0.82
0.80	1.03	0.91	1.17	0.97	1.20	0.85	0.78
1.90	2.01	1.31	2.42	-0.35	2.79	1.41	-4.22
1.07	0.90	1.14	0.97	1.21	0.99	1.25	0.73
1.10	0.92	1.18	0.98	1.22	0.97	1.24	0.70
2.83	1.95	3.07	1.22	0.53	-2.16	-0.02	-4.31
0.94	1.15	0.97	1.25	-	1.31	-	0.59
0.93	1.19	0.97	1.27	-	1.35	-	0.58
-1.78	3.89	0.08	1.24	-	3.39	-	-1.44
1.15	0.98	1.21	-	1.35	1.20	0.96	
1.19	0.98	1.22	-	1.29	1.17	0.93	
3.77	0.74	0.36	-	-3.97	-2.46	-3.27	
0.94	1.17	0.99	1.31	1.20	0.85	0.70	
0.94	1.21	0.98	1.35	1.17	0.83	0.68	
0.08	3.26	-0.87	3.19	-2.83	-2.49	-2.79	
1.27	0.88	1.25	-	0.96	0.70		
1.28	0.87	1.25	-	0.93	0.69		
1.13	-0.33	0.79	-	-3.57	-2.42		
0.78	0.82	0.73	0.59				
0.77	0.80	0.70	0.57				
-1.41	-2.36	-4.47	-3.07				

Rel. Diff [%]	
Max	-4.47
Min	-0.02
RMS	2.41

BEA VRS
MCS
Rel. Diff. [%]

Fig. 15. Axially integrated detector signal at the BOC (step 1).

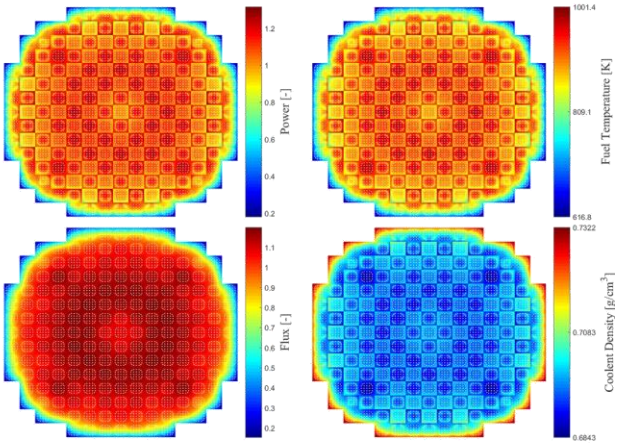

Fig. 16. Axially integrated quantities at the MOC (step 15): power, flux, fuel temperature, and coolant density.

-	1.06	1.30	1.11	1.28	1.02	1.16	0.66
-	1.04	1.31	1.10	1.28	1.02	1.19	0.66
-	-1.28	0.27	-0.93	0.28	0.12	2.56	-0.14
1.06	1.29	1.11	1.30	1.09	-	0.83	0.67
1.03	1.28	1.10	1.32	1.08	-	0.83	0.66
-2.55	-0.85	-1.18	1.07	-0.71	-	-0.44	-1.00
1.30	1.11	1.32	1.11	1.26	1.01	1.12	0.61
1.31	1.09	1.33	1.09	1.28	1.01	1.16	0.62
0.31	-1.95	0.62	-1.91	1.62	-0.11	2.94	1.79
1.11	1.30	1.11	1.30	-	1.21	-	0.50
1.10	1.34	1.09	1.29	-	1.22	-	0.49
-0.60	2.58	-1.50	-0.60	-	0.69	-	-2.18
1.28	1.09	1.26	-	1.09	1.00	0.72	
1.28	1.06	1.27	-	1.10	0.99	0.71	
0.45	-2.12	1.03	-	0.64	-0.15	-1.39	
1.02	-	1.01	1.21	1.00	0.70	0.53	
1.02	-	0.99	1.22	1.00	0.69	0.52	
-0.29	-	-1.76	1.37	0.45	-0.97	-0.73	
1.16	0.83	1.12	-	0.72	0.53		
1.18	0.83	1.14	-	0.71	0.53		
1.84	-0.74	1.39	-	-0.68	0.81		
0.66	0.67	0.61	0.50				
0.66	0.67	0.61	0.49				
0.37	-0.02	0.32	-1.25				

Rel. Diff [%]	
Max	2.94
Min	-0.02
RMS	1.29

BEA VRS
MCS
Rel. Diff. [%]

Fig. 17. Axially integrated detector signal at the MOC (step 15).

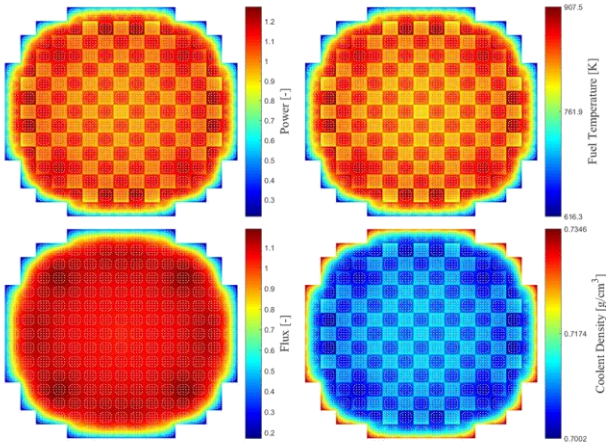

Fig. 18. Axially integrated quantities at the EOC (step 23): power, flux, fuel temperature, and coolant density.

-	-	1.17	1.05	1.20	1.06	1.20	0.68
-	-	1.18	1.03	1.25	1.08	1.23	0.70
-	-	0.52	-1.56	3.97	1.25	2.48	2.28
-	1.18	1.03	1.17	1.07	-	0.93	0.70
-	1.20	1.03	1.21	1.05	-	0.92	0.70
-	1.09	-0.46	2.72	-1.07	-	-1.70	-0.45
1.17	1.03	1.20	1.06	1.23	1.08	1.16	0.66
1.18	1.03	1.20	1.06	1.23	1.07	1.20	0.65
1.20	-0.05	0.20	-0.25	0.77	-0.82	4.12	-1.93
1.05	1.17	1.06	1.24	-	1.25	-	0.55
1.03	1.20	1.05	1.24	-	1.26	-	0.52
-2.13	2.26	-0.72	-0.14	-	1.11	-	-4.91
1.20	1.07	1.23	-	1.13	1.11	0.76	
1.23	1.06	1.23	-	1.13	1.08	0.76	
2.69	-0.35	-0.02	-	0.35	-2.12	0.08	
1.06	-	1.08	1.25	1.11	0.82	0.57	
1.08	-	1.06	1.26	1.08	0.78	0.55	
1.17	-	-1.76	1.37	-2.51	-5.16	-3.10	
1.26	0.93	1.16	-	0.76	0.57		
1.22	0.92	1.20	-	0.75	0.54		
-3.17	-1.52	4.19	-	-1.68	-4.95		
0.68	0.70	0.66	0.55				
0.69	0.72	0.65	0.52				
1.65	1.49	-1.46	-6.16				

Rel. Diff [%]	
Max	-6.16
Min	-0.02
RMS	2.38

BEA VRS
MCS
Rel. Diff. [%]

Fig. 19. Axially integrated detector signal at the EOC (step 23).

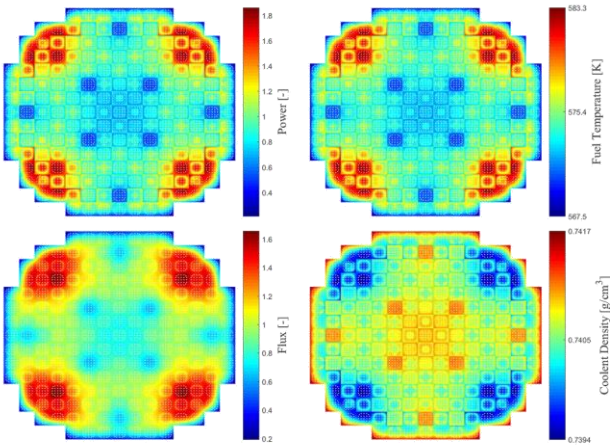

Fig. 20. Axially integrated quantities at the step 2: power, flux, fuel temperature, and coolant density.

-	0.52	1.02	0.99	1.24	0.91	0.81	0.70
-	0.75	1.05	0.92	1.15	0.85	0.72	0.62
-	45.00	2.46	-7.10	-6.54	-7.07	-11.12	-11.37
0.52	0.92	0.89	1.36	1.19	1.47	0.76	0.89
0.76	0.98	0.80	1.13	0.98	1.19	0.77	0.71
46.43	5.83	-10.17	-17.37	-17.78	-19.33	1.90	-20.46
1.02	0.89	0.39	0.63	1.94	0.53	1.55	0.41
1.04	0.81	0.69	0.93	1.32	1.06	1.26	0.72
1.90	-8.63	75.83	48.27	-31.76	101.01	-18.22	76.05
0.99	1.36	0.63	0.74	-	1.11	-	0.78
0.92	1.15	0.94	1.35	-	1.59	-	0.66
-7.38	-15.79	49.05	81.50	-	42.70	-	-15.81
1.24	1.19	1.94	-	3.61	0.52	1.42	
1.19	0.98	1.33	-	1.59	1.44	1.13	
-4.00	-17.48	-31.50	-	-55.95	175.18	-20.35	
0.91	1.47	0.53	1.11	0.52	0.54	0.80	
0.84	1.17	1.07	1.60	1.46	1.04	0.85	
-7.32	-20.07	102.89	43.73	177.89	92.19	5.79	
0.81	0.76	1.55	-	1.42	0.80		
0.73	0.77	1.29	-	1.14	0.87		
-10.90	1.55	-16.71	-	-20.16	8.09		
0.70	0.80	0.41	0.78				
0.62	0.71	0.73	0.64				
-11.14	-10.47	78.62	-17.60				

Rel. Diff [%]	
Max	177.89
Min	1.55
RMS	52.27

BEAVRS
MCS
Rel. Diff. [%]

Fig. 21. Axially integrated detector signal at the step 2.

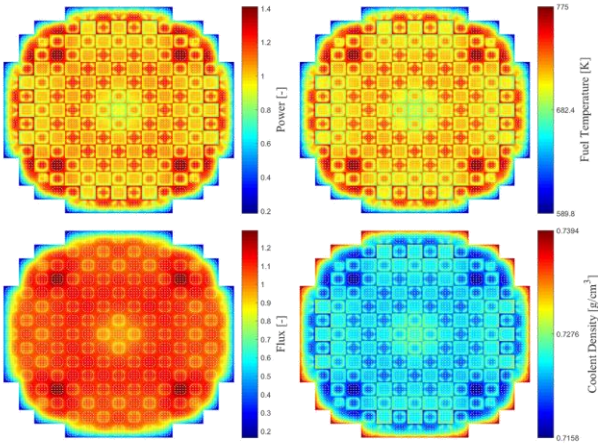

Fig. 22. Axially integrated quantities at the step 6: power, flux, fuel temperature, and coolant density.

-	0.96	1.30	0.56	1.31	0.98	1.27	0.71
-	0.90	1.28	1.02	1.24	0.94	1.25	0.70
-	-6.00	-1.82	80.88	-5.23	-3.83	-1.32	-1.68
0.96	1.26	1.07	1.33	1.05	1.27	0.81	0.76
0.89	1.21	1.02	1.28	1.00	1.22	0.81	0.72
-6.92	-3.80	-4.88	-3.56	-4.59	-3.41	-0.20	-5.74
1.30	1.07	1.34	1.06	1.28	0.84	1.22	0.67
1.24	1.01	1.30	1.03	1.27	0.96	1.19	0.64
-4.48	-5.44	-2.58	-2.42	-1.31	14.10	-1.96	-3.53
0.56	1.33	1.06	1.16	-	1.29	-	0.53
1.00	1.29	1.03	1.30	-	1.28	-	0.52
77.19	-3.08	-2.83	12.27	-	-0.44	-	-1.92
1.31	1.05	1.28	-	1.23	-	0.80	
1.26	1.00	1.27	-	1.18	-	0.79	
-3.84	-4.39	-1.26	-	-3.83	-	-0.37	
0.98	1.27	0.84	1.29	-	0.70	0.60	
0.96	1.22	0.96	1.28	-	0.72	0.58	
-2.15	-3.40	14.05	-0.60	-	2.35	-4.09	
1.27	0.81	1.22	-	0.80	0.60		
1.22	0.83	1.22	-	0.80	0.58		
-3.23	3.03	0.06	-	-0.04	-3.56		
0.71	0.76	0.67	0.53				
0.69	0.71	0.65	0.53				
-2.23	-6.27	-3.33	-1.58				

Rel. Diff [%]	
Max	80.88
Min	-0.04
RMS	16.65

BEAVRS
MCS
Rel. Diff. [%]

Fig. 23. Axially integrated detector signal at the step 6.

IV. REMAINING ISSUES

BEAVRS benchmark cycle 1 simulation was performed with assumptions and simplifications without quantifying the impacts of them. The impacts of the following assumptions and simplification will be studied in the future.

- The fuel was divided into only 10 axial meshes. It may be required to use finer meshes.
- A closed channel simple TH solver was used. It may be possible to improve the results by coupling with CTF.
- The cross-section broadening effect was considered only for the 72 nuclides in the resonance range. The nuclides other than those 72 nuclides may affect the results significantly.
- The thermal scattering law data, and unresolved resonance energy cross-section (PTable) were not broadened.
- Equilibrium xenon number density was used. The power changes frequently, and the xenon number density should be calculated considering power history.
- The TH feedback strategy needs further verification.

V. CONCLUSIONS

The preliminary solution of BEAVRS cycle 1 depletion was presented in this paper. The simulation was performed with five feedback modules: TH, depletion, equilibrium xenon, CBC, and the OTF cross-section broadening. The CBC and detector signal map were compared with the measured data in the benchmark specification. It was shown that the MCS can estimate the CBC within the maximum 100 ppm difference, and MCS can calculate detector signal within about 2-5% error in most case. There are few assumptions and simplifications used in this simulation without quantifying the effect of them. In the future, each of them will be further studied.

ACKNOWLEDGMENTS

The authors would like to acknowledge Prof. Han Gyu Joo of SNU and nTRACER development team for sharing TH module implemented in the nTRACER, and Prof. Ben Forget of MIT and OpenW development for sharing OpenW code & library.

This work was supported by the National Research Foundation of Korea (NRF) grant funded by the Korean government (MSIP) (NRF-2014M2A8A1032045)

REFERENCES

1. H. Lee, W. Kim, P. Zhang, A. Khassenov, Y. Jo, and D. Lee, “Development Status of Monte Carlo Code at UNIST,” KNS Spring Meeting, Jeju, Korea, May 12-13, (2016).
2. H. Lee, C. Kong, and D. Lee, “STATUS OF MONTE CARLO CODE DEVELOPMENT AT UNIST,” Proc. PHYSOR 2014, Kyoto, Japan, Sep 28–OCT 28, 2014, American Nuclear Society, (2014).
3. M. Ryu, et al., “Solution of the BEAVRS benchmark using the nTRACER direct whole core calculation code,” Journal of Nuclear Science and Technology, 52, pp. 961-969, (2014).
4. C. Josey, P. Ducru, B. Forget, and K. Smith, “Windowed multipole for cross section Doppler broadening,” Journal of Computational Physics, (2015).
5. A. Khassenov, S. Choi, and D. Lee, “On the Fly Doppler Broadening Using Multipole Representation,” KNS Spring Meeting, Jeju, Korea, May 7-8, (2015).
6. F. B. Brown, MCNP – A General Monte Carlo N-Particle Transport Code, Version 5, LA-UR-03-1987, Los Alamos National Laboratory, (2003).
7. T. Goorley, et al., Initial MCNP6 Release Overview, Nucl. Technol., 180, pp 298-315, (2012).
8. A. Isotalo, J. Leppanen, J. Dufek, “Preventing xenon oscillations in Monte Carlo burnup calculations by enforcing equilibrium xenon distribution,” Annals of Nuclear Energy, 60, 78-85, (2013).
9. F. Yang, et. Al., “IMPLEMENTATION OF INLINE EQUILIBRIUM XENON METHOD IN RMC CODE,” PHYSOR 2016, Sun Valley, ID, May 1-5 (2016).
10. N. Horelik, and et. al, MIT benchmark for evaluation and validation of reactor simulations (BEAVRS), Version 2.0, MIT: MIT Computational Reactor Physics Group, (2016).